

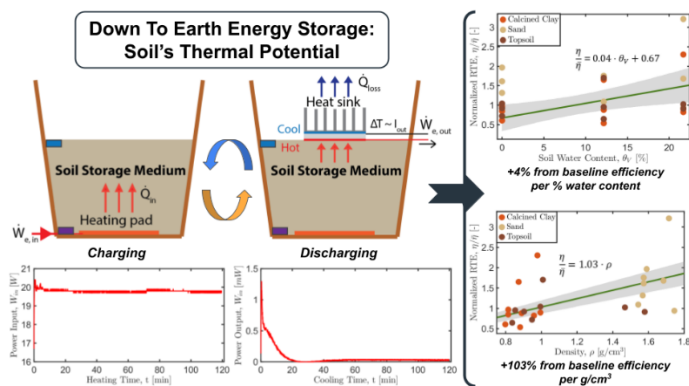
THE EFFECTS OF SOIL PROPERTIES ON THERMAL BATTERY EFFICIENCY

Josiah Shimandle

MIT Department of Mechanical Engineering

Cambridge, MA, USA

VISUAL ABSTRACT



0. ABSTRACT

Soil can provide a low-cost medium for thermal energy storage in off-grid communities where energy sources are often intermittent, and other methods of energy storage are often neither accessible nor scalable. However, the difference in performance of soil-based thermal storage across different soil types is not well understood. Three soil types with varying water content were tested as thermal storage media across three identical thermal batteries. Temperature gradients were measured during charging and discharging cycles, and round-trip efficiency was calculated from measured input and output power. Across soil types, soil density was found to have a significant positive effect on thermal battery efficiency, while soil water content has a similar positive effect on efficiency due to its positive correlation with density. These findings suggest that selecting for or otherwise increasing the density of soil by adding water and compaction, can improve the efficiency of soil-based thermal storage.

Keywords: Thermal battery efficiency, sensible heat storage, thermal properties of soil, sand batteries, microgrid energy.

1. INTRODUCTION

Amidst global decarbonization efforts, sustainable, low-cost methods of energy storage are necessary to accommodate the inconsistency of renewable energy sources such as solar and wind. For this reason, thermal energy storage is a growing topic of interest in industry and academic research as a sustainable method of long-term energy storage [1]. Thermal batteries are composed of three main components as shown in Figure 1: an energy source, a thermal storage medium, and an energy delivery method. Energy is typically provided to the storage media through either solar or electrical heating. Thermal energy can then be discharged from the battery through heat exchanger flow or, in some contexts, through radiation. Material choice for a thermal battery's storage medium plays an important role in determining the capacity of the battery. In industry, clay bricks, sand, graphite blocks, molten salt, and phase change materials are all popular choices for thermal storage media because of their high heat capacity and ability to withstand high temperatures [2]. In addition to holding more energy, operating at a higher temperature can allow thermal batteries to operate more efficiently during the discharging process [3]. Large scale thermal batteries operating at temperatures upwards of 1500 °C have been reported by industry leaders to store thermal energy at efficiencies as high as 98% [4].

Natural soil is also often used as a medium for thermal storage in small-scale domestic applications such as greenhouse heating [5]. Natural materials such as clay, sand, and other forms of soil are uniquely accessible in rural contexts, where access to grid energy is often unreliable. The use of soil for thermal storage can provide a sustainable, low-cost solution to the challenge of unreliable energy access in rural communities. Soil provides a distinct advantage over water, another low-cost thermal storage medium, in terms of scalability as the design of water-based thermal storage is often constrained

by the size of commercially available water tanks and storage temperatures cannot exceed the boiling point of water. The existing body of literature on soil-based thermal storage focuses primarily on sand and clay as these are the soils most prevalent in industry. Soil properties are complex, especially for soils that fall between the two extremes of sand and clay, where organic and inorganic materials mix. Considering this, a quantifiable understanding of thermal battery performance across the full range of soil types from sand to silt to clay, would be a particularly useful tool to those seeking to lessen their reliance on the grid through thermal battery technology.

In order to understand the impact of different soil-based thermal media on thermal battery performance, topsoil, sand, and calcined clay were mixed with varying amounts of water and then tested as thermal storage media across a full charging and discharging cycle. The round-trip efficiency for each battery and soil was then calculated and compared with the density and soil water content of three different types of soil acting as the thermal storage media. Density and soil water content were used as characteristic properties of each soil because of their well-established relation to soil's thermal properties [6]. Efficiency was calculated from the measured power input and output of each thermal battery across the cycle of charging and discharging. Measured efficiencies were then blocked by battery and plotted against the measured soil water content and density of each battery's medium to determine if there was any significant relationship between the measured soil properties and battery efficiency. The temperature gradient within each battery was measured in order to characterize the thermal properties of each soil during the charging and discharging process.

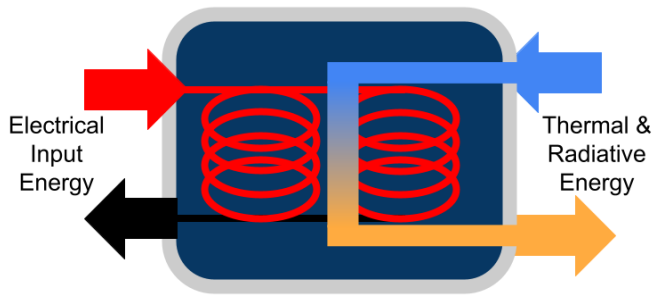


Figure 1: A typical industrial thermal battery design. The thermal storage medium is shown in dark blue, with grey insulative walls. Electrical energy is input to the system via resistive heating. Energy is discharged from the battery as thermal energy through a heat exchanger or as radiative energy through an open window in the insulation.

2. BACKGROUND

Soil-based thermal batteries are a specific subset of the broader thermal battery technology. In this way, as with a typical thermal battery, the performance of soil-based thermal storage can be understood as dependent on the properties of soil in as much as they define the fundamental performance parameters of the battery: capacity and efficiency.

2.1 HEAT TRANSFER IN SOILS

The USDA Natural Resource Conservation Service considers soil to be composed of three primary inorganic particles: sand, silt, and clay. Soils are typically classified by their texture, which describes the ratio of sand, silt, and clay present in the soil. Sand is the largest of these three particles while clay is the smallest. Clay and silt tend to hold water well while sand is highly permeable. Due to their difference in particle size, soils with a high clay content are typically denser than those with a high sand content [7].

The thermal conductivity and specific heat capacity of soil can be highly variable within soil types and has been shown to vary with both soil depth and time of day [8]. Previous studies have shown that thermal conductivity of soil to be positively related to bulk density and water content. One study found thermal conductivity ranging from 0.42 to 0.85 $\frac{W}{m \cdot K}$ for loamy soil, representative of most topsoil, in a central Iowa field [9]. Specific heat capacity in soils is generally considered to be primarily a function of density and water content. Previous studies have shown that the specific heat capacity of soils can range from 0.83 $\frac{kJ}{kg \cdot K}$ for dry sand to 2.25 $\frac{kJ}{kg \cdot K}$ for wet clay [6]. Heat capacity tends to be higher in soils with a high clay content due to clay's high density and water holding properties. There is a range of existing research on the effects of soil density and water content on soil thermal properties, but few studies relate these thermal properties to applications in thermal storage [10].

Studies show conduction to be the dominant mode of heat transfer in soils across different levels of moisture content, with thermal conductivity generally being higher for soils with greater moisture content [11]. The analytical basis for conduction in soil, as with most solids, is Fourier's law of thermal conduction, shown in Equation (1), which states that local heat flux density q_x is equal to the negative of the product of the thermal conductivity k and the local temperature gradient ∇T .

$$q_x = -k\nabla T. \quad (1)$$

In addition to analytical models, heat transfer has been effectively examined in the literature with numerical models of conduction that have been experimentally shown to be valid [12].

2.2 THERMAL BATTERY PERFORMANCE

One of the primary measures of performance for thermal batteries is heat capacity, which is the amount of energy that can be stored in the battery for each degree increase in temperature. The specific heat capacity of a material is the amount of energy it takes to heat up 1 kg by 1 °C. By this definition the total amount of energy that can be stored in a thermal battery can be calculated with Equation (2), where Q is equal to the product of the specific heat capacity c , the mass m , and the increase in temperature ΔT of the thermal storage medium.

$$Q = cm\Delta T. \quad (2)$$

In addition to heat capacity, efficiency, η , is key measure of thermal battery performance. η is the ratio of energy delivered from the battery to energy stored in the battery during one cycle of charging and discharging, as shown in Equation (3). One study, examining sand-based thermal storage systems for residential applications through numerical models, predicted round trip efficiencies as low as 20%, which was found to be primarily due to the degradation of insulation surrounding the storage medium [13].

$$\eta = \frac{W_{out}}{W_{in}}. \quad (3)$$

In practice it is generally desirable for thermal batteries to operate at very high temperatures while remaining well insulated as this increases both the energy density of the battery and the efficiency with which it operates. Energy can be delivered from thermal batteries directly as heat transfer, or as electrical energy through turbines or generators, but in both these cases the process of discharging energy is typically more efficient across a large temperature gradient [3].

3. EXPERIMENTAL DESIGN

In order to capture the full range of soil properties, calcined clay, topsoil, and sand were selected to be tested as thermal storage media at varying water content levels. Samples of these three soil types are shown in Figure 2. Three identical makeshift thermal batteries were constructed with a given soil mixture as a storage medium. Each makeshift thermal battery contained a 20 W heating

pad placed at the bottom of a 10 cm diameter clay pot. This pot was wrapped with aluminum foil to capture an insulating pocket of air and limit radial heat transfer through the pot walls, ensuring the dominant mode of heat transfer within the battery was in the axial direction, towards the upper surface of the soil. One thermocouple was placed at the base of the pot, and a second thermocouple was placed 4.2 cm above it to be approximately in line with the upper surface of the soil, as shown in Figure 3. Three identical batteries were constructed to allow for tests to be run in parallel. For each trial, 360 mL of soil was measured and packed into one of these insulated clay pots to be heated and subsequently cooled. The mass of each sample of soil was measured before testing in order to calculate the corresponding density. Water was added to soil samples in varying amounts, 0%, 12%, and 22% water content by volume.



Figure 2: Dried samples of calcined clay, topsoil, and sand, from left to right as tested.

3.1 HEATING

During heating, a controlled DC power input was sent to the heating pad and measured through a digital “watts up? PRO” power meter for a period of two hours. This time period was chosen to ensure each test reached steady state operation before discharging. Temperature data was recorded via two Vernier thermocouples placed at the base and surface of the soil, in order to quantify the time-dependent thermal gradient in the soil during the charging and discharging process.

3.2 COOLING

After the two hour period of charging, the input power was switched off and a Hilitand thermoelectric generator (TEG) was pressed onto the surface of the soil. A TEG is a device that generates electrical current proportional to the temperature difference between its two faces. TEGs are notoriously inefficient devices, but were chosen for use in this study because they allow for a precise quantification of power output from the thermal battery in the form of electrical work. An aluminum heat sink was attached

pasted to the upper surface of each TEG to accelerate the cooling and increase the temperature differential and corresponding power output of the device. Each TEG was then wired in series to a resistor that was matched to its optimal load resistance, $R_L = 5 \Omega$.

R_L was chosen to match the internal resistance, R_{TEG} , of the model of TEG being used. $R_{TEG} \approx 4.1 \Omega$ was calculated experimentally according to Equation (4), where V_{oc} is the measured open-circuit voltage, and I_{sc} is the measured short-circuit current. This result was then verified experimentally by testing the power generated by the TEG under different load resistances, and it was confirmed that the TEG generated maximum current with $R_L = 5 \Omega$ when compared with 2.5Ω and 10Ω resistors.

$$R_{TEG} = \frac{V_{oc}}{I_{sc}}. \quad (4)$$

After placing the TEG onto the surface of the soil, the output current and corresponding electrical work was measured for a period of two hours, ensuring each battery was fully cooled. Temperature data was collected at the surface and base of the soil for the entire cooling process. This cycle of heating and cooling was repeated between two and four times for each of the nine combinations of clay, sand, or topsoil with 0%, 12%, or 22% water content.

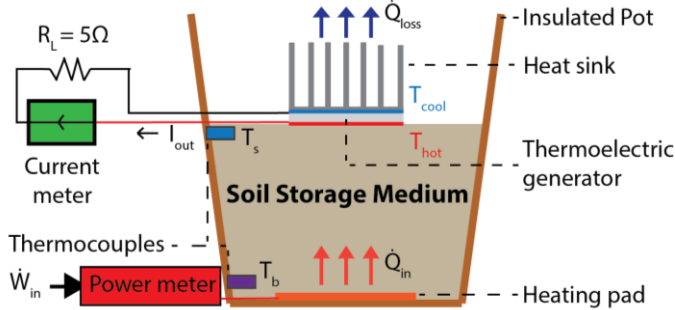


Figure 3: Makeshift test battery with measured power input through heating pad and measured power output through TEG. Note that the TEG was only placed onto the soil during cooling and was not present for heating.

4. RESULTS AND DISCUSSION

4.1 THERMAL PROPERTIES OF SOIL

Temperature data was collected for every test at the surface and at the base of the battery in order to determine the temperature gradient within the storage medium during the heating and cooling process. During heating, both temperatures initially increased in a nearly linear fashion, until heat loss to the environment increased and the

temperature difference between the base and surface of the battery approached a steady state equilibrium, ΔT_{eq} . Cooling followed a similar pattern of rapid initial cooling and attenuation to a fully cooled steady state.

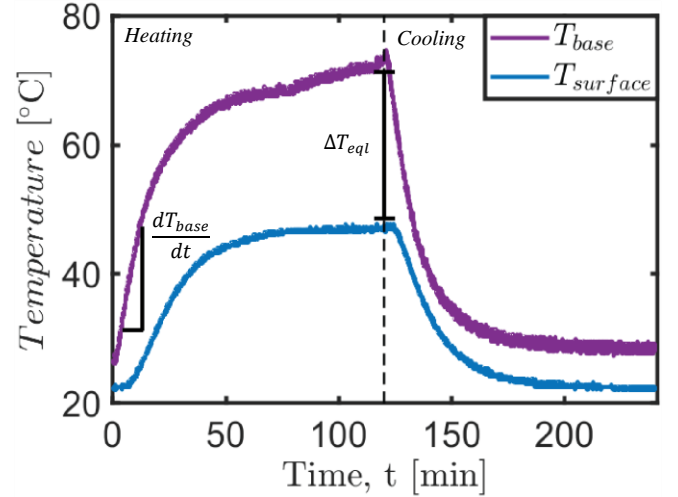


Figure 4: Thermocouple data from the heating and cooling of calcined clay with 12% water content. The rate of change of the base temperature within the initial linear regime, $\frac{dT_{base}}{dt}$, is marked as the slope of the purple line. The end of heating and beginning of cooling is marked at 120 min, and the corresponding equilibrium temperature difference between the surface and base of the battery is marked as the distance between the purple and blue lines at that time, ΔT_{eq} .

The measured temperature data were used to estimate the thermal properties of each soil type used. At the beginning of heating, heat loss to the environment was considered to be negligible. Accordingly, the temperature at the base of the battery, closest to the heating pad increases in a roughly linear fashion with respect to time. Heat capacity was then calculated for each test using Equation (2) according to $\frac{dT_{base}}{dt}$ within the linear heating regime, assuming a constant heat input $\dot{W}_{in} = 20 [W]$.

Thermal conductivity was calculated according to Equation (1), Newton's law of cooling in the axial direction. Radial heat transfer was neglected as the walls of each pot were assumed to be well insulated. The thermal gradient within the battery was determined based on the difference in equilibrium temperature between the surface and base of the battery, ΔT_{eq} , as shown in Figure 4, divided by the distance between thermocouples, $L = 4.2 \pm 0.2 \text{ cm}$. The heat flux at equilibrium, q_x , for each test was determined from Equation (5) based on the measured heat

input rate \dot{W}_{in} and the area of the pot's upper surface $A = 79 \pm 5 [cm^2]$. A general estimate of heat capacity and thermal conductivity was calculated for each soil type by averaging calculated values across all tests for a given soil type.

$$q_x = \frac{\dot{W}_{in}}{A}. \quad (5)$$

Although uncertainty was large for most estimates of soil thermal properties, as shown in Figure 5, the estimates for specific heat capacity all fit within the typical range of values for soil in general as suggested by the literature, between 0.83 to $2.25 \frac{kJ}{kg \cdot K}$ [5]. The estimates for thermal conductivity however are much larger than expected based on the literature which suggests values nearly an order of magnitude less than what was calculated [9]. This overestimate of thermal conductivity would suggest that the assumption neglecting radial heat loss in the makeshift battery may not be entirely valid.

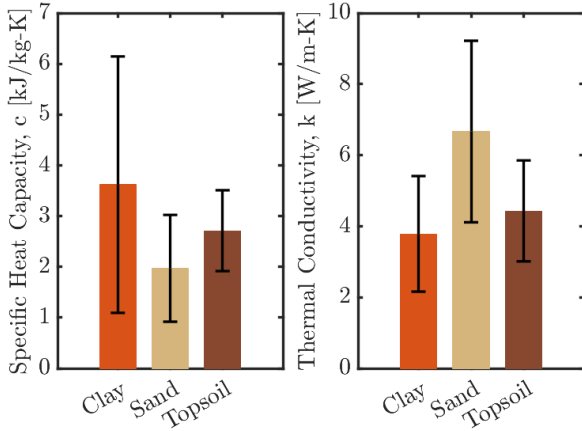


Figure 5: Empirically determined specific heat capacity, c , (left) and thermal conductivity, k , (right) of calcined clay, sand, and topsoil calculated from temperature data during heating process.

4.2 BATTERY PERFORMANCE

In order to calculate efficiency for each test, the total electrical work input and output to the system were measured. Power input via the heating pad was directly measured during testing. The electrical power output \dot{W}_e was calculated as the product of the load resistance R_L with the square of the electrical current, I , as seen in Equation (6).

$$\dot{W}_e = I^2 R_L. \quad (6)$$

In this manner the time-varying power output from the thermal battery via the TEG was calculated from the measured current output and known load resistance $R_L = 5$ and is shown together with the time-varying power input in Figure 6.

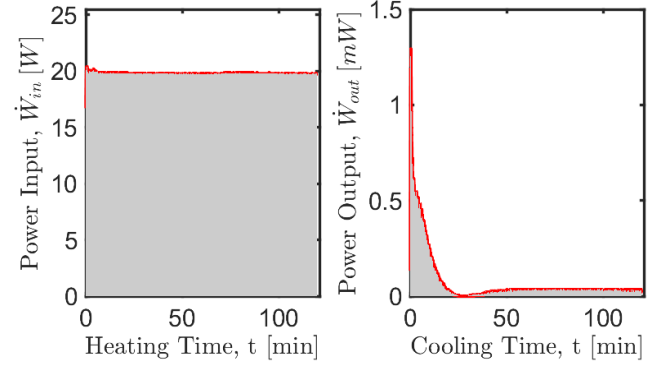


Figure 6: Time varying power input (left) and power output (right) for calcined clay with 12% water content. The shaded area under each curve represents the total electrical work into and out of the battery respectively.

Total work input and output to the battery can be found by integrating the power input and output over the period of heating and cooling respectively as seen in Equation (7).

$$E = \int_{t_i}^{t_f} \dot{W}(t) dt. \quad (7)$$

Round-trip efficiency, η , was calculated as the ratio of work out to work in, as seen in Equation (3). η was then plotted against soil water content, θ_v , and density, ρ , as shown in Figure 7. A linear fit was chosen to model the relationship between η and θ_v . This fit showed no significant impact of θ_v on η . A proportional fit was chosen to model the relationship between η and ρ on the physical basis that no efficiency is possible for a medium with no density. This fit showed a small but significant impact of ρ on η equal to an increase of $(1.8 \pm 0.6) \times 10^{-3} \left[\frac{\%}{g/cm^3} \right]$. Compared to any useful battery, the efficiencies of the soil-based thermal batteries tested were very low, on average $\eta_{avg} = (1.9 \pm 0.4) \times 10^{-3} [\%]$. These low efficiencies are due primarily to the combined effects of poor insulation and the inherent inefficiency of discharging thermal energy across small temperature gradients.

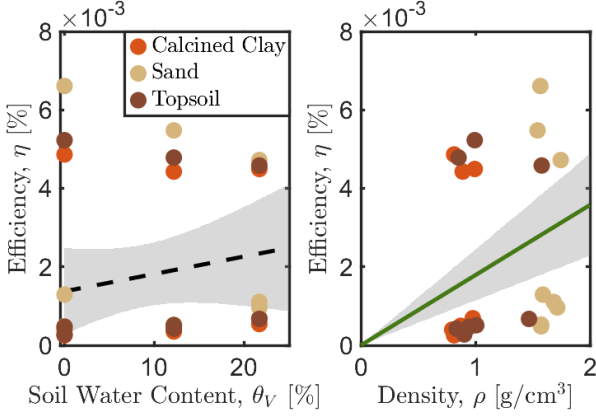


Figure 7: Efficiency, η , as correlated with soil water content, θ_V , (left) and density, ρ , (right) for each tested cycle. The proportional fit $\eta = C_\rho \cdot \rho$ is shown on the right in green with the 95% confidence interval highlighted in grey. The slope of this line, $C_\rho = (1.8 \pm 0.6) \times 10^{-3} \left[\frac{\%}{\text{g/cm}^3} \right]$, represents the percentage point increase in η for a $1 \frac{\text{g}}{\text{cm}^3}$ increase in ρ . The linear fit $\eta = C_\theta \cdot \theta_V$ was not significant, and is shown on the left as a dotted black line.

As is evident from Figure 7, the spread of efficiencies is quite large and bimodal, due to variations in performance between the three different TEGs used. In order to take into account the effects of these difference in TEG efficiency between the three different battery setups, these data were blocked according to the particular TEG used during testing and a normalized efficiency, η^* , was calculated for each test as defined in Equation (8), where $\bar{\eta}$ is the average efficiency across all tests where the same TEG was used.

$$\eta^* = \frac{\eta}{\bar{\eta}}. \quad (8)$$

This η^* was calculated for each individual test and was plotted against θ_V and ρ of the soil storage medium as shown in Figure 7. A linear fit was again used to model the impact of θ_V on efficiency, which showed a significant impact of θ_V on η^* with a leading coefficient $C_\theta^* = 0.037 \pm 0.027 [-]$. This suggests that for a 10 % increase in θ_V , actual efficiency, η , will experience a percentage point increase equal to 38 ± 27 % of the average reference efficiency, $\bar{\eta}$.

A proportional fit was again chosen to model the impact of ρ on efficiency. A significant positive relationship was found between η^* and ρ , with a leading coefficient of $C_\rho^* = 1.03 \pm 0.2 \left[\frac{\text{cm}^3}{\text{g}} \right]$. This suggests that

for a $1 \frac{\text{g}}{\text{cm}^3}$ increase in ρ , actual efficiency, η , will experience a percentage point increase equal to 103 ± 2 % of the average reference efficiency, $\bar{\eta}$.

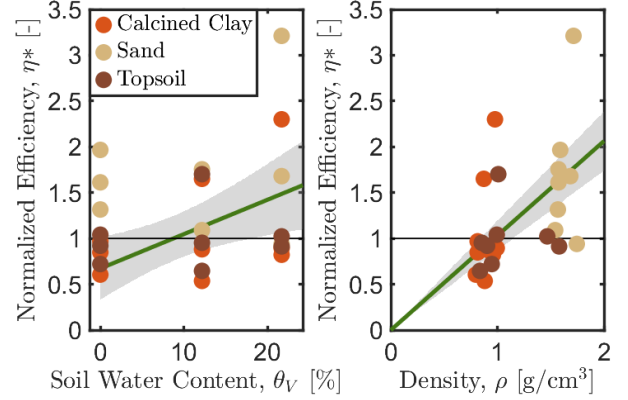


Figure 8: Normalized efficiency, η^* , as correlated with soil water content, θ_V , (left) and density, ρ , (right) for each tested cycle. The proportional fit $\eta^* = C_\rho^* \cdot \rho$ is shown on the right in green with its 95% confidence interval highlighted in grey. The slope of this line, $C_\rho^* = 1.03 \pm 0.2 \left[\frac{\text{cm}^3}{\text{g}} \right]$, represents the percent increase of η^* from its average value, marked at $\eta^* = 1$, for every added $\frac{\text{g}}{\text{cm}^3}$ of density. The linear fit $\eta^* = C_\theta^* \cdot \theta_V + a_\theta$ is shown similarly on the left with its 95% confidence interval. The slope of this fit, $C_\theta^* = 0.038 \pm 0.027 [-]$, similarly represents the percent increase of η^* from 1 for every percent increase in soil water content.

The impact of θ_V on η can be assumed to be in part due to its correlation with ρ . As shown in Figure 9, there is a significant positive correlation between soil density and water content, equal to an increase in ρ of $0.03 \pm 0.02 \left[\frac{\text{g}}{\text{cm}^3} \right]$ for a 1 % increase in θ_V . This suggests that density is the overarching parameter affecting efficiency in this context.

Higher density soil is generally considered preferable for thermal storage because of its higher heat capacity. The finding that increasing density also increases the efficiency of the storage process reinforces this understanding that higher density storage media lead to better performance in thermal batteries overall. This positive effect is suggestive of methods that could be employed to improve soil-based thermal battery efficiency even without changing the type of soil used as a media, for example packing soil manually to increase its density within the battery.

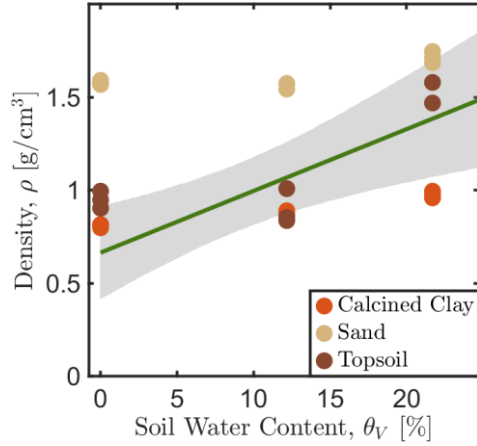


Figure 9: Soil density, ρ , plotted against water content, θ_V , for tested soil-based storage media. A linear fit $\rho = C_{\rho\theta} \cdot \theta_V$ shown as the green line, demonstrates a positive relationship between ρ and θ_V , equal to a density increase of $C_{\rho\theta} = 0.03 \pm 0.02 \left[\frac{g}{cm^3} \right]$ for a 1 % increase in soil water content.

While these results demonstrate a significant impact of soil density and water content on the efficiency of this particular thermal battery design, it is not clear whether these results will persist for batteries operating under different conditions. In practice, thermal batteries are most practical if operated under higher temperatures and with larger storage volumes than were considered. In addition, the mechanism by which density increases efficiency was not precisely determined and is something worth exploring further. Future research in this area should focus on differentiating the many particular parameters density might be affecting which allow it to increase efficiency. Furthermore, the behavior of thermal batteries across many cycles of charging and discharging is of great practical importance when considering their performance in the long-term, although this cyclic behavior was not directly considered in these results. Future studies should examine the behavior of soil-based thermal batteries at full scale, operating under typically useful conditions and over repeated cycles, in order to better understand these effects in a practical context.

5. CONCLUSIONS

Although the overall efficiencies of the thermal batteries tested were quite low, the results revealed important relationships that could inform the design of more practical soil-based thermal storage systems. For a $1 \left[\frac{g}{cm^3} \right]$ increase in density, round-trip efficiency increased by $103 \pm 2 \%$ of the average efficiency of the given

battery setup. This effect is relatively small for batteries operating under inherently inefficient conditions, but for well insulated batteries operating at high temperatures, these gains in efficiency could lead to substantial gains in efficiency for only modest increases in the density of the storage medium. Similarly, for a 10 % increase in soil water content, round-trip efficiency increased by $38 \pm 27 \%$ of the average efficiency of the given battery setup. This positive effect of water content on efficiency seems to be primarily due to its positive impact on soil density, but for practical purposes still stands as a useful mechanism for improving the efficiency of soil storage media.

These findings have significant practical implications for rural communities seeking to implement low-cost thermal storage solutions. Intentional selection of high-density soils, compaction, and the addition of water could all enhance the performance of soil-based thermal storage media. These gains scale with the average efficiency of the particular storage and discharge method. For this reason, these relatively simple steps could lead to substantial gains in efficiency for thermal batteries that are well insulated and operating at a high temperature. Future research should focus on elucidating the specific mechanisms by which density affects efficiency and exploring how these relationships scale with better insulation and higher operating temperatures.

ACKNOWLEDGMENTS

The author would like to thank Dr. Barbara Hughey for her tireless support in the design, execution, and analysis of this project, Kevin DiGenova for his guidance and encouragement throughout, Ian Shimandle for his assistance in the processes of ideation and proofreading, and Prof. Dan Frey for his patient and thoughtful advising and for the generous lending of 3, 5 Ω power resistors.

REFERENCES

- [1] Sun, Mingyang, Tianze Liu, Xinlei Wang, Tong Liu, Mulin Li, Guijun Chen, and Dongyue Jiang. 2023. "Roles of Thermal Energy Storage Technology for Carbon Neutrality." *Carbon Neutrality*, 2 (1) (12): 12. doi:https://doi.org/10.1007/s43979-023-00052-w.
- [2] Crownhart, C., 2024. "How to build a thermal battery," MIT Technology Review. https://www.technologyreview.com/2024/04/18/1091481/how-to-build-a-thermal-battery/.
- [3] Yong Cao, Liangping Dong, Yafeng Deng, Hongyan Liu, Chenyang Gao, Xiaowei Yang, Chao Wang, Yanhua Cui. 2021. "Working temperature maintenance of thermal batteries by using a slow heat

supply component with layer structure and its positive effect on the improvement of electrochemical performance,” *Composites Part B: Engineering*, 222. <https://doi.org/10.1016/j.compositesb.2021.109036>.

Repository. DOI: <https://doi.org/10.22215/etd/2023-15714>.

- [4] Rondo Energy. 2023. “Rondo Energy announces world’s highest temperature thermal energy storage,” [rondo.com](https://www.rondo.com/news-press/rondo-energy-announces-worlds-highest-temperature-thermal-energy-storage) [Online]. Available: <https://www.rondo.com/news-press/rondo-energy-announces-worlds-highest-temperature-thermal-energy-storage>.
- [5] Mousavi Ajarostaghi, Seyed Soheil, Leyla Amiri, and Sébastien Poncet. 2024. "Application of Thermal Batteries in Greenhouses" *Applied Sciences*, 14, no. 19: 8640. <https://doi.org/10.3390/app14198640>.
- [6] Nidal H. Abu-Hamdeh. 2003. “Thermal Properties of Soils as affected by Density and Water Content,” *Biosystems Engineering*, 86 (1): 97-102.
- [7] USDA Soil Science Division Staff. 2021. “Soil Survey Manual”, United States Department of Agriculture Handbook No. 18.
- [8] Romio, Leugim Corteze, Tamires Zimmer, Tiago Bremm, Lidiane Buligon, Dirceu Luis Herdies, and Dé Roberti. 2022. "Influence of Different Methods to Estimate the Soil Thermal Properties from Experimental Dataset." *Land*, 11 (11): 1960. [doi:https://doi.org/10.3390/land11111960](https://doi.org/10.3390/land11111960).
- [9] Tong, Bing, Dilia Kool, Joshua L. Heitman, Thomas J. Sauer, Zhiqiu Gao, and Robert Horton. 2020. "Thermal Property Values of a Central Iowa Soil as Functions of Soil Water Content and Bulk Density Or of Soil Air Content." *European Journal of Soil Science* 71 (2) (03): 169-178.
- [10] Nusier, Osama & Abu-Hamdeh, Nidal. 2015. “The Effect of Water Content and Bulk Density on Specific Heat and Volumetric Heat Capacity of Sand and Loam Soils.” *Sylwan*, 158.
- [11] Wang R, Yang C, Ni L, Yao Y. 2020. “Experimental study on heat transfer of soil with different moisture contents and seepage for ground source heat pump.” *Indoor and Built Environment*, 29 (9): 1238-1248.
- [12] Tawfiq Chekifi, Moustafa Boukraa. 2023. “CFD applications for sensible heat storage: A comprehensive review of numerical studies,” *Journal of Energy Storage*, 68.
- [13] Pinto, Rebecca Ingrid. 2023. “Modelling and Experimental Evaluation of a Sand-Based Seasonal Storage System,” *Carleton University Institutional*